

UNCLASSIFIED

Defense Technical Information Center
Compilation Part Notice

ADP012635

TITLE: Thin Films of Antimony-Tin Oxide as Counter-Electrodes for Proton Working Electrochromic Devices

DISTRIBUTION: Approved for public release, distribution unlimited

This paper is part of the following report:

TITLE: Progress in Semiconductor Materials for Optoelectronic Applications Symposium held in Boston, Massachusetts on November 26-29, 2001.

To order the complete compilation report, use: ADA405047

The component part is provided here to allow users access to individually authored sections of proceedings, annals, symposia, etc. However, the component should be considered within the context of the overall compilation report and not as a stand-alone technical report.

The following component part numbers comprise the compilation report:
ADP012585 thru ADP012685

UNCLASSIFIED

Thin Films of Antimony-Tin Oxide as Counter-Electrodes for Proton Working Electrochromic Devices

N. Naghavi, C. Marcel, L. Dupont, A. Rougier and J-M. Tarascon

Laboratoire de Réactivité et Chimie des Solides, Université de Picardie Jules Verne, 80039 Amiens Cedex.

ABSTRACT

We report here on thin films proton-working electrochromic devices based on the well-known tungsten oxide as the coloring electrode, and Antimony Tin Oxide (ATO) as the ion-storage counter-electrode. We show that films deposited by Pulsed Laser Deposition (PLD) technique have an apparent Sb solubility up to 70 at %, and exhibit unusual electrochromic properties. Through potentiostatic tests we'll demonstrate that depending on the composition which influences film morphology, the Sn-Sb-O films could either present a faradic or a capacitive-like behavior, associated to a color or a neutral switching over a wide range of potentials, respectively. The structural properties of ATO films are characterized by X-ray diffraction and transmission electron microscopy (TEM). Electrochromic behavior is studied by means of cyclic voltamperometry coupled with *ex situ* optical transmittance measurements in the visible range. The maximum proton-storage capacity is observed for ATO films containing 40-50 at % Sb, while being quasi-neutral when switching over a wide range of potentials. These compositions are finally retained for the assembly of our WO₃/proton-electrolyte/ATO devices, whose performances are reported.

INTRODUCTION

In recent years, owing to their capability of persistent and reversible color changes under a reversible electrochemical process, electrochromic materials have been widely involved in optical technology, particularly in the field of display panels, antiglare car rear-view mirrors and transmission modulation through building windows [1,2]. To ensure a large-scale development for this energy conscious architecture, the cost of smart windows needs to be lowered, especially for proton-working devices, which are easier to build than lithium conducting ones. Until now, the most durable all-solid inorganic system is composed of tungsten oxide as the cathodically colored working electrode and iridium [3] as the complementary counter-electrode, both components exchanging proton ions. However, owing to the high cost of iridium oxide, research has turned on cheaper electrochromic materials such as hydrous nickel oxide [4]. But the latter also presents non-negligible drawbacks such as a poor stability in acidic electrolytes. Thus, a need for alternative and economical materials, which can be used in the composition of proton-conducting electrochromic devices, remained in order to constitute an ion-storage for WO₃, and keep the same optical density over cycling. Based on our previous works we will show that the Sn-Sb-O system may effectively satisfy that need [5].

EXPERIMENTAL DETAILS

Thin oxide films were prepared by pulsed laser deposition using a KrF excimer laser beam (Lambda Physic, Compex 102, $\lambda=248$ nm) with a laser fluence of 1-2 J/cm². The targets

were pellets of commercial SnO₂ (Aldrich 99.9%) and Sb₂O₃ (Aldrich 99.9%) mixtures in stoichiometric proportions annealed for 20 h at a relatively low temperature (700 °C) in order to avoid any antimony loss while achieving a pellet density of 60-70%. Films of 1*1 cm² area were deposited either onto (SnO₂:F)-coated glass for electrochemical tests or onto simple glass for structural and electronic characterizations. Deposition time was fixed at 15 min with a repetition rate of 3 Hz. The thickness, determined by profilometry using a Dektak St instrument, was estimated as being in the range of 200-250 nm.

Film crystallinity was examined by X-ray diffraction (XRD) with a Philips diffractometer model PW 1710 (λ CuK α = 0.15418 nm). High-resolution transmission electron microscopy (HRTEM) was carried out using a JEOL 2010 microscope equipped with an energy-dispersive X-ray spectroscopy (EDS) analyzer.

Optical transmission spectra in the UV-visible and near infrared regions (250-2500 nm) were obtained using a Varian double beam, UV-Vis-NIR spectrometer "CARY-5E".

The electrochemical properties of the films were characterized by cyclic voltammetry performed with an Autolab PGSTAT 30 system. The cell consists of the ATO film as the working electrode and of a platinum wire as the counter electrode, both immersed in a 0.1M aqueous H₃PO₄ electrolyte. The potentials were given versus the saturated calomel electrode (SCE) reference. For all these experiments, cyclic voltammograms (CV) were scanned at a rate of 10 mV/s.

RESULTS AND DISCUSSION

Films of various antimony-tin oxide compositions were grown from targets whose nominal composition was ranging between 0 and 80 at.% Sb. More specifically, the films were deposited at 200 °C under 10⁻⁷ mbar oxygen pressure, then annealed for 30 min at 550 °C under the same oxygen pressure, and then characterized for their electrochromic properties. Under such deposition conditions, as deduced from EDS analysis, we noted that the Sn/Sb atomic ratio was relatively well preserved between target and grown films.

Structural characterizations:

Figure 1 shows the X-ray diffraction patterns of ATO thin films deposited on glass substrate, which are typical of SnO₂ cassiterite phase. Increasing Sb amount yields a loss of crystallinity; this trend being also observed for ATO thin films deposited on FTO substrate. The absence of peaks pertaining to antimony oxide phases (whatever the oxidation states) lets suppose the complete dissolution of antimony in the nanostructured SnO₂. Beyond 70% Sb, films become amorphous. At first such results could indicate that the "apparent solubility limit" of antimony in nanocrystalline tin oxide is reached near the 70% Sb.

At this point a legitimate question was whether these Sb-enriched ATO specimens were presenting large amounts of amorphous antimony-containing material as previously reported [6] or they were single phases. To unambiguously answer such a question, HRTEM measurements were carried out on our heavily substituted ATO films.

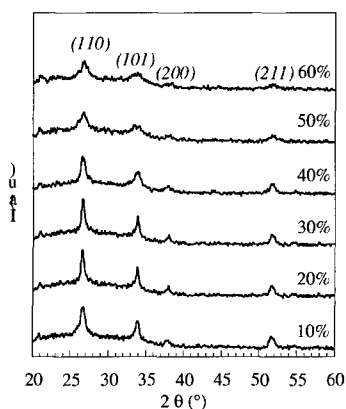


Figure 1: X-ray diffraction patterns of ATO thin films with $10 \leq \%Sb \leq 60$ having a SnO_2 -Cassiterite structure.

Figs. 2. a. and b. display HRTEM micrographs of films deposited from targets composed of 40% Sb and 60% Sb, respectively.

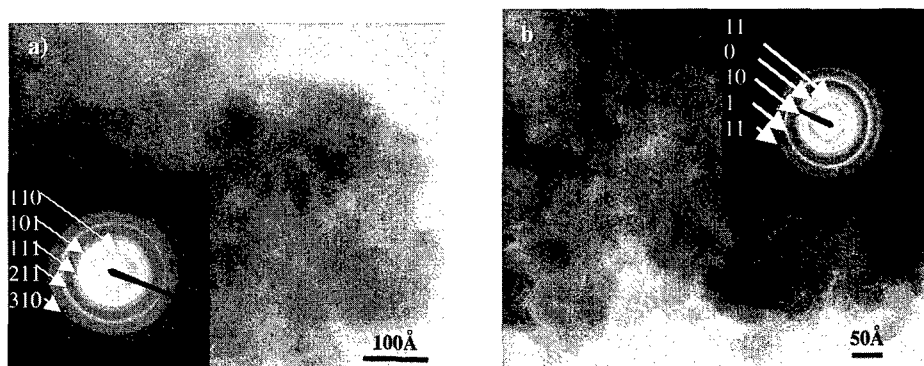


Figure 2: TEM micrographs of ATO thin films with composition of a) 40% Sb and b) 60% Sb.

The high-resolution images and the electron diffraction patterns recorded from these materials gave no evidence for the presence of any antimony oxide phase. For both compositions the diffraction pattern contains well-resolved diffraction rings characteristic of SnO_2 cassiterite phase. Indeed, films consist of small disordered crystals of a cassiterite-type solid, and no trace of amorphous materials is observed independently of antimony amount. However, changes in film texture with composition are visible: while the film with the lowest antimony content (40% Sb, Fig. 2. a.) is very dense, and exhibits a poor definition of particle shape, the film containing 60% Sb (Fig. 2. b.) appears less dense with better defined grains of about 50 Å. In short, the TEM study confirmed the formation of Sn-Sb-O solid solution with a SnO_2 cassiterite-type structure up to a concentration of 60% Sb.

Electrochemical characterizations:

Cyclic voltammograms (CV's) of our ATO films were obtained by sweeping the potential from (-0.7 to 1.5V) vs. SCE. Depending on the film Sb content two apparent types of CV traces were observed (Fig. 3). Within the 10-40% Sb range, CV curves are featureless, and the transmittance remains the same as shown for the (60%Sn-40%Sb) sample in Fig. 3. c. As the antimony contents increases up to 50%, the cyclic voltammogram of the films adopts a pseudo-capacitive like shape as previously shown by Marcel et al.⁵

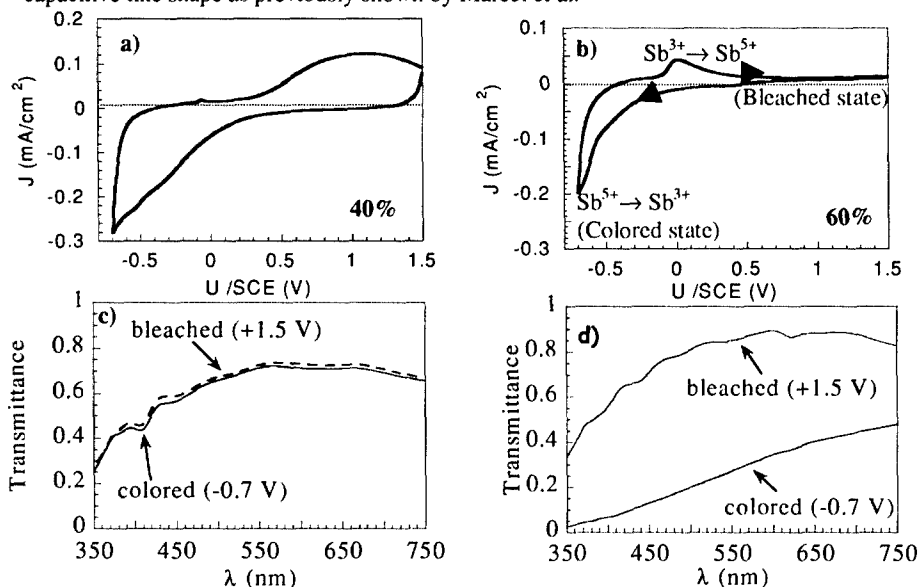


Figure 3: Voltammograms of (a) 60%Sn-40%Sb and (b) 40%Sn-60%Sb thin films. CV's were recorded between -0.7 and 1.5 V vs. SCE with a sweep rate of 10 mV/s. Optical transmittance spectra of thin films of compositions (c) 60%Sn-40%Sb and (d) 40%Sn-60% Sb, bleached at 1.5 V, and cathodically colored at -0.7 V.

From 60 to 70% Sb content, a pronounced faradic behavior appears, possibly corresponding to ($Sb^{5+} \leftrightarrow Sb^{3+}$) charge transfer with simultaneous H^+ (dc) intercalation. Indeed a redox couple, visible at ca. 0V in oxidation and -0.7V in reduction, produces a dark-gray coloration with the cathodic sweep, followed by a bleaching process with anodic one. Increasing Sb amount reinforces the optical contrast (Fig. 3. d.) for the composition (40% Sn-60% Sb).

For specimens having a capacitive-like behavior (typically those containing 40% Sb) we noted that the charge density increased with cycling. The origin of this cycling-driven activation is most likely nested in the non-granular film nature that limits the proton diffusion, as neither the surface morphology nor the thickness were modified after cycling. In fact TEM measurements on films containing 40% Sb show no real change in their morphology after cycling about 100 times. These films remain very dense which may lead to a slow proton

diffusion and a capacitive behavior of these films. On the other hand, films with composition $\geq 60\%$ Sb lost their capacity after cycling. After about 100 cycles, TEM micrographs indicated a loss of density associated to a better grain definition, which may facilitate the proton diffusion leading to their "perfect" faradic behavior. Suggesting that these films tend to slightly dissolve in H_3PO_4 electrolyte, the resulting cycling lifetime is apparently short. The electrolyte was modified by either changing the concentration or its nature so as to minimize film dissolution.

Another interesting result is that the best charge density per micron thickness (volumic capacity) was obtained over the 40-60% Sb range. The best volumic capacity and the optically neutral trend of ATO 40%, make it a good candidate to be used as a counter electrode switching against the preferment electrochromic electrode, i.e. WO_3 .

An ATO-based device was so tested in H_3PO_4 (0.1 M) liquid electrolyte. Three-electrode measurements were carried out using WO_3 as the working electrode and ATO (40% Sb) as the counter electrode, first investigating the potential evolution vs the exchanged charge density for each component, then studying the stability of coloration and bleaching processes. We saw that ATO is not limiting, while the equilibrium potentials are stable for colored and bleached states. Therefore ATO (40%) is a reliable counter electrode for proton switching.

Two sorts of proton-conducting solid electrolyte were considered: A hydrated Ta_2O_5 solid electrolyte and a polymer (H_3PO_4 -doped PBI ($x=1$) gel) electrolyte. Here we will only present results for the first one.

WO_3 and $\text{Ta}_2\text{O}_5/\text{ATO}$ half-cells were grown separately on FTO/glass substrate using PLD, and their respective thickness was adjusted so that their capacities were balanced. The WO_3 film was deposited at RT in 10^{-1} mbar O_2 pressure ($t_{\text{WO}_3}=3000 \text{ \AA}$), whereas the ATO film was deposited as previously indicated ($t_{\text{ATO}}=5000 \text{ \AA}$), and Ta_2O_5 deposited on top with the same oxygen pressure of 10^{-2} mbar at $200 \text{ }^\circ\text{C}$ ($t_{\text{Ta}_2\text{O}_5}= 2000 \text{ \AA}$). WO_3 was first H^+ -preinserted (blue coloration) in H_3PO_4 (0.1 M) liquid electrolyte with a charge density of 15 mC/cm^2 , the stack $\text{Ta}_2\text{O}_5/\text{ATO}$ was cycled in the same medium in order to check its ion-storage ability. Finally the whole cell was assembled using epoxy resin.

Two-electrode potentiostatic measurements were first carried out in order to check if the pre-inserted amount of proton was effectively exchanged by the device (Fig. 5. a). Note that the scan rate was considerably reduced compared to the liquid electrolyte medium (1 mV/s) in order to enable each component to react with proton. Then optical measurements were operated through the whole cell (Fig. 5. b). Indeed for the electrochromism application, the amount of inserted species (i. e. Capacity) is not the main parameter but is linked to the resulting optical contrast yielding a figure of merit expressed by the coloration efficiency (CE)². This coloration efficiency CE is expressed as the ratio between the contrast in the bleached state (T_b) and the colored state (T_c) and the charge density (Q). See equation 1.

$$\text{CE} = (1/Q) * \log (T_b/T_c) \quad (1)$$

These measurements are yielding coloration efficiency of $35 \text{ cm}^2/\text{C}$ for our device, which is about the same as that of WO_3 half-cell. Thus ATO is an effective optically passive counter electrode. However this value can be improved whilst the overall transmission is considerably lowered by FTO/glass and ATO layers, and can be improved by using pigments such as TiO_2 .

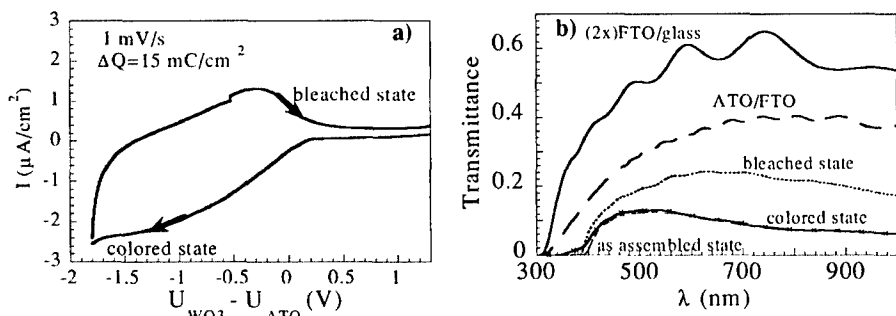


Figure 4: (a) Voltammograms of a two-electrode $\text{WO}_3/\text{Ta}_2\text{O}_5/\text{ATO}$ system. CV's were recorded between -1.8 V and 1.5 V vs. SCE with a sweep rate of 1 mV/s. (b) optical transmittance spectra of the device bleached at 1.5 V, and cathodically colored at -1.8 V.

CONCLUSION:

In summary, through a systematic study of Sn-Sb-O thin films, we gave evidence for a direct relationship between the ATO thin film electrochromic behavior and morphology via changes in Sb content. Based on a charge transfer between Sb^{3+} and Sb^{5+} , the optical contrast between bleached/colored states is thus dictated by the antimony concentration in tin oxide matrix. It increases to the detriment of electrochemical stability, which yields the most antimony-rich compositions (60-70% Sb) presenting a typical faradic behavior to be non-suitable proton-conducting switching electrodes. On the other hand, films containing 40% Sb present a neutral coloration over a wide potential scale associated to a capacitive-like behavior and a good capacity retention. These features make them good candidates in their use as cheap counter electrodes in proton-working devices. The feasibility of an all-solid electrochromic window constituted by WO_3 blue-switching electrode exchanging H^+ ions with an ATO film containing 40% Sb was studied. This device was assembled using Ta_2O_5 electrolyte. An electrochromic coloration efficiency of about 35 cm^2/C was so obtained, which is about the same as that of WO_3 half-cell. Thus ATO is an effective optically passive counter electrode. However, in order to improve the transmission of such a system, and increase its switching time there is a need to improve the proton conduction for the electrolyte, and try to enlight ATO counter-electrode with pigments such as TiO_2 .

REFERENCES:

1. P. M. S. Monk, R. J. Mortimer, D. R. Rosseinsky, in *Electrochromism Fundamentals and Applications* (VCH, New York, 1995).
2. C. G. Granqvist, *Handbook of Inorganic Electrochromic Materials*, (Elsevier, Amsterdam, 1995).
3. M. A. Petit, V. Plichon, *J. Electroanal. Chem.*, **444**, 247 (1998).
4. A. Azens, L. Kullman, G. Vairars, H. Nordborg, C. G. Granqvist, *Solid State Ionics* **449**, 113 (1998).
5. C. Marcel, M. S. Hegde, A. Rougier, C. Maugy, C. Guéry, J. M. Tarascon, *Electrochem. Acta*, **46**, 2097 (2001).
6. F. J. Berry, D. J. Smith, *J. Catal.*, **88**, 107 (1984).